# Practical and Sensitive Measurement of Methane Gas Concentration Using a 1.6 µm Vertical-Cavity-Surface-Emitting-Laser Diode

Seiichi Kakuma[*] and Kazutoshi Noda[1]

Division of Applied Physics, Graduate School of Engineering, Hokkaido University
N13W8, Kita-ku, Sapporo, Hokkaido 060-8628, Japan
[1]Institute for Environmental Management Technology,
National Institute of Advanced Industrial Science and Technology (AIST),
AIST Tsukuba West, 16-1 Onogawa Tsukuba, Ibaraki 305-8569, Japan

Methane ($CH_4$)-based natural gas is increasingly being used as city gas. Since $CH_4$ gas is explosive, accurate and sensitive $CH_4$ gas concentration sensors are required. We have developed practical and sensitive equipment for measuring the methane gas concentration based on infrared (IR) absorption by sweeping light with a 1.6 µm wavelength emitted from a vertical-cavity-surface-emitting-laser diode (VCSEL). This method can be used to measure the $CH_4$ concentration with a resolution better than 0.1% and is unaffected by the wavelength drift of the light source.

## 1. Introduction

From the viewpoint of reducing carbon dioxide ($CO_2$) emission, it is anticipated that the use of natural gas, mainly composed of methane ($CH_4$), will continue to increase in future. Since $CH_4$ is flammable and explosive, it is widely recognized that the development of practical and sensitive systems for detecting $CH_4$ gas concentration is necessary for gas management. The main systems currently used for $CH_4$ measurement are as follows: catalytic combustion systems,[1] semiconductors,[2] thermal conduction systems,[3] interferometers,[4] and infrared (IR) absorption systems.[5–14] Among these systems, only IR absorption systems are capable of measuring trace gas concentrations without being affected by other gases.

In IR absorption systems, distributed feedback laser diodes (DFB-LDs) have been employed by several researchers[7–14] because of their wavelength tunability, compactness, availability, and maintenance-free operation. The wavelength of a DFB-LD can be easily tuned by controlling temperature and drive current, the tunable range

[*]Corresponding author: e-mail: kakuma@eng.hokudai.ac.jp

of which is approximately from 0.5 to 0.1 nm.  Since the tunable range is approximately an order of magnitude smaller than the wavelength spacing of absorption lines of $CH_4$ gas, the screening of DFB-LDs with respect to their tunable region has been required to ensure the detection of an absorption line.

The recent development of vertical-cavity-surface-emitting-laser diodes (VCSELs) provides us with an attractive LD for IR absorption methods.  VCSELs can perform wavelength tuning with a range of up to about 5 nm by current control with a width of only 3 mA or less.  Since this tunable range exceeds the wavelength spacing of the absorption lines of $CH_4$, the initial screening and the selection of VCSELs are not required.  In addition, the high-speed current control makes it possible to use synchronous detection technique; thus, the change in the amplitude of the absorption line can be detected in real time with high sensitivity.

In this paper, we describe the basic theory of the system fabricated using a VCSEL and its experimental setup, and demonstrate its utility by presenting experimental results for the detection of trace concentrations of $CH_4$.

## 2.   Basic Principle of Gas Concentration Measurement Using IR Absorption

The IR absorption method can selectively detect a gas using a narrow absorption line that appears in its specific absorption spectrum.  From the HITRAN database,[15] the absorption lines of $CH_4$ are clustered around wavelength bands at 1,300, 1,600, 3,300, and 7,700 nm, and optical absorption generally increases with increasing optical wavelength.  Among these bands, the 1,600 nm absorption band is adopted in our measurement system, because of the following advantages: there is greater absorption at 1,600 nm than at 1,300 nm, the lack of interference from the absorption lines of water vapor ($H_2O$), and the availability of optical parts and devices with lower cost than those used for 3,300 and 7,700 nm bands.  The absorption bands and their maximum absorption intensities are summarized in Table 1, and the absorption lines around 1,600 nm are shown in Fig. 1.[15]

When a gas absorbs incident light at a specific wavelength number $v$ (cm$^{-1}$), the relation between the optical intensity of the transmitted light and the incident light is described by the Lambert-Beer law,[16]

Table 1
IR absorption bands of CH4 and their maximum absorption intensities.

| Absorption band (μm) | Maximum absorption intensity (atm$^{-1}$ cm$^{-2}$) |
| --- | --- |
| 1.3 | $3.7 \times 10^{-3}$ |
| 1.6 | $3.3 \times 10^{-2}$ |
| 3.3 | 5.3 |
| 7.6 | 2.4 |
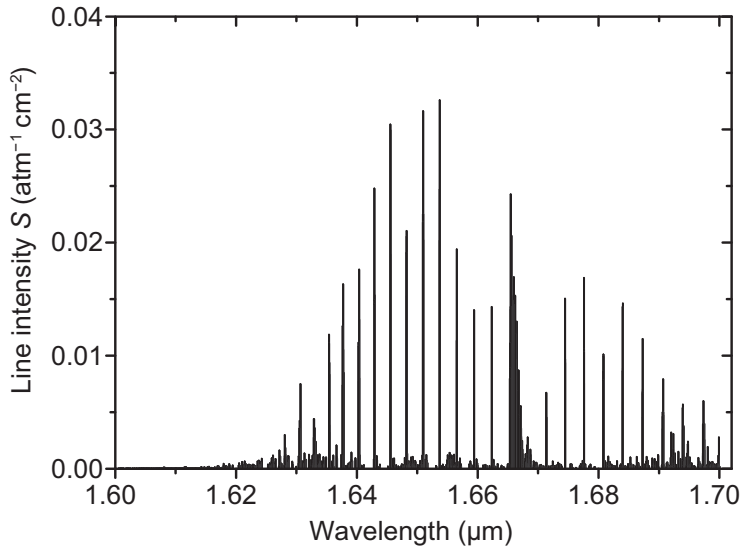
Fig. 1.   Absorption lines of $CH_4$ in 1.6 μm band.

$$I/I_0(v) = \exp[-\alpha(v)L], \tag{1}$$

where $I_0$, $I$, $\alpha(v)$, and $L$ are the intensities of the incident light and transmitted light, the absorption coefficient (cm$^{-1}$), and the gas cell length (cm), respectively.  The absorption coefficient $\alpha(v)$ is related to the gas concentration $C$ (%) by

$$\alpha(v) = PCX\Phi(v), \tag{2}$$

where $P$, $S$, and $\Phi(v)$ are the pressure (atm), line intensity (atm$^{-1}$ cm$^{-2}$), and absorption line profile (cm), respectively.  At lower concentrations, where $\alpha(v)L \ll 1$ is satisfied, the absorption ratio $K$ is approximated as

$$K = 1 - I/I_0 = 1 - \exp[-\alpha(v)L] \approx \alpha(v)L. \tag{3}$$

The concentration $C$ is theoretically estimated by substituting the value of $\alpha(v)$ into eq. (2), where $\alpha(v)$ is numerically determined from the measured value of $K$.  However, the actual values of $P$, $S$, and $\Phi(v)$ are generally unknown.  We, therefore, experimentally determine the relationship between $K$ and $C$, where the values of $C$ are calibrated using other measuring tools in advance.  This relationship gives the analytic line for concentration measurements.

## 3.    Concentration Measurement by 2*f*-Synchronous Detection

### 3.1    *Experimental system*

Figure 2 shows the basic experimental setup of the proposed system.  The lasing wavelength of a VCSEL depends on the operation temperature of the chip and its drive current, both of which are used to tune the wavelength in our system.  The temperature is controlled and stabilized by an electronic temperature control system with a thermoelectric element, and the wavelength is coarsely tuned to one of the absorption lines of $CH_4$.  After the coarse tuning, the absorption line profile is detected by sweeping the wavelength repeatedly around the line with triangular current modulation (repetition frequency $f$ =1 kHz).

The output beam from the VCSEL is collimated by an objective lens and is divided into two beams.  One of the beams is input to a gas cell (length $L$ = 20 cm) and the triangular intensity change of the transmitted beam is detected by photodiode (PD)1 (Hamamatsu Photonics Inc.: Type G8421-05).  The same intensity change detected by PD2 is used as a signal to monitor the VCSEL output.  By adjusting the amplitude of the triangular signal from PD2 so that it is equal to that of PD1 using a preamplifier, the absorption profile induced by $CH_4$ gas in the cell can be detected as the difference between the two signals by a differential amplifier.  Consequently, the differential signal is observed as a 2*f*-frequency signal, as shown in Fig. 3.

The ability to detect the absorption signal is limited by the noise component included in both triangular signals.  We therefore used the synchronous detection technique with a
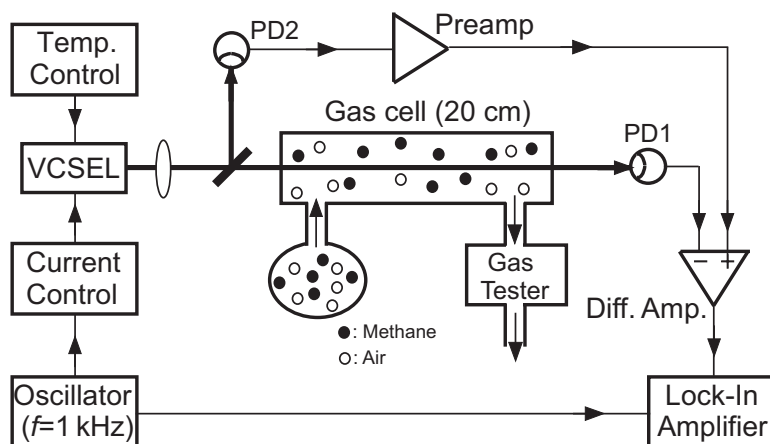


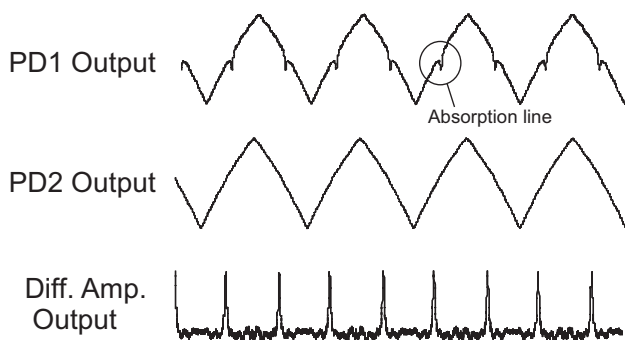Fig. 2.    Experimental setup of the 2*f* detection system.

Fig. 3.   Triangular intensity variations detected by PD1 and PD2, and the differential signal.

lock-in amplifier to improve the signal-to-noise ratio of measurements.  This is achieved by adjusting the absorption line in the center of each up/down slope of every triangular waveform.  The adjustment is made by the fine control of the bias current of the VCSEL, and the amplitude of the differential signal is detected by the lock-in amplifier in the $2f$ reference mode.

In the experiments, we produced $CH_4$ gas samples consisting of standard $CH_4$ gas (99%) mixed with air, and the concentration of each sample calibrated by a gas tester of an optical-interference type (R7, Hokkaido Toka Fine Technique Co., Ltd.).

### 3.2   *Experimental results of 2f detection technique*

Figure 4 shows the analytic line determined by measurements of concentrations ranging from 0 to 4.5%.  The lock-in amplifier output increases in proportion to $CH_4$ concentration.  However, the concentration output deviates from the analytic line in the long term, because the absorption line gradually shifts from its initial position on the triangular intensity line owing to the central-wavelength drift of the VCSEL.  As shown in Fig. 5, two effects are simultaneously induced by the wavelength drift; the deviation of frequency from $2f$ and the change in absorption line amplitude.  The former appears as a reduction of the lock-in output independent of the direction of the wavelength shift direction, whereas the output change due to the latter factor is dependent on the direction of the shift.  The wavelength shift is attributed to the temperature drift of the VCSEL chip.  Although the temperature of the VCSEL is stabilized by the thermoelement, large fluctuations of environmental temperature readily cause errors in the control, resulting in unexpected temperature drifts of the VCSEL.

Figure 6 shows the measured changes in output voltage (at 3.5% $CH_4$) induced by the temperature drift of the VCSEL.  Output voltage decreases from 8 to 2 V when temperature deviates from the initial temperature of 43.6°C by 0.5°C.  Referring to the analytic line in Fig. 4, the decrease in output corresponds to the reduction of $CH_4$
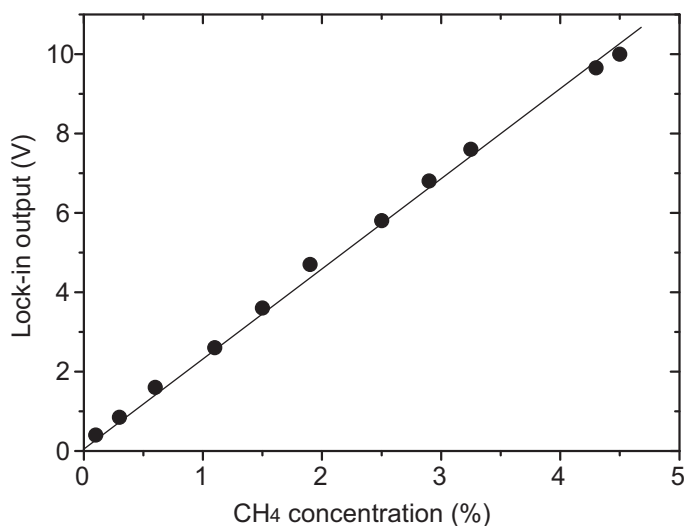
Fig. 4.   Analytic line of CH$_4$ concentration (0 to 4.5%) obtained by the 2$f$ detection system.
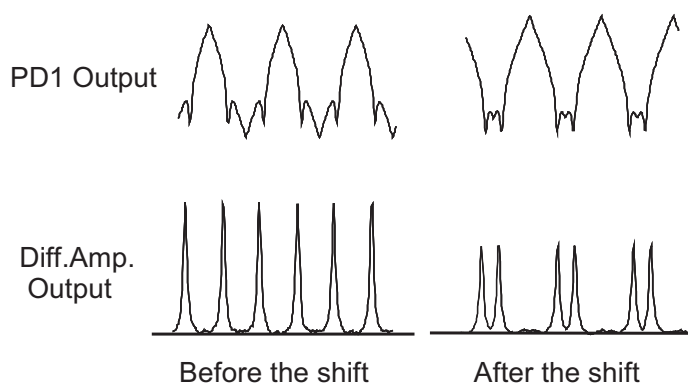


Fig. 5.   Comparison of differential signal waveforms before and after the absorption line shift of the PD1 output.

concentration from 3.5 to 0.9%.  Also, the output is maximized at the initial temperature, which indicates that the deviation of frequency from 2$f$ is the main cause of the deviation of the output.   These results show that the wavelength shift of the VCSEL during measurement is problematic in the 2$f$ method.
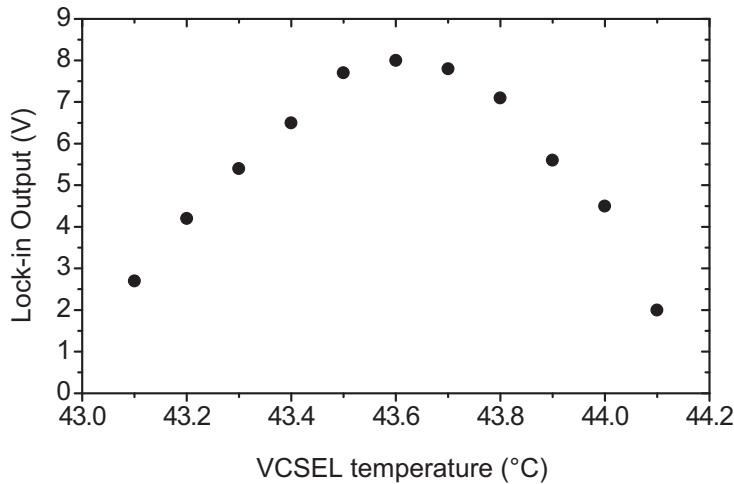
Fig. 6. Measured output voltage of the lock-in amplifier plotted as a function of VCSEL temperature.

## 4. Real-Time Measurement System Using *f*-Synchronous Detection

To resolve the above-mentioned difficulty, we have developed an approach consisting of synchronously detecting either the up or down signal with the frequency *f* and normalizing the amplitude of the absorption line using the simultaneously monitored intensity.

### 4.1 *Experimental system*

Figure 7 shows the experimental setup of the *f* system. Its optical configuration is the same as that used in the 2*f* detection technique. The generator outputs a rectangular signal synchronously with the triangular voltage used for modulation of the VCSEL (*f* = 1 kHz). After being inverted, the rectangular signal is added to the differential signal including the absorption line profile. As shown in Fig. 8, the absorption profiles are extracted as positive parts of the combined signal by the ideal diode circuit; thus, the absorption profiles can be synchronously and stably detected using the reference frequency *f*. Simultaneously, the output from the ideal diode circuit is divided by the output from PD2 using an analog divider (Fig. 9). Because the profile signal is normalized, the lock-in output is also unaffected by the change in amplitude of the absorption line induced by the wavelength drift of the VCSEL.

### 4.2 *Experimental results and discussion*

An experimentally obtained analytic line is shown in Fig. 10, the data for which was acquired when VCSEL temperature was controlled (at 43.6°C) in such a way that each absorption line is adjusted to the center of the modulated up/down line. Using
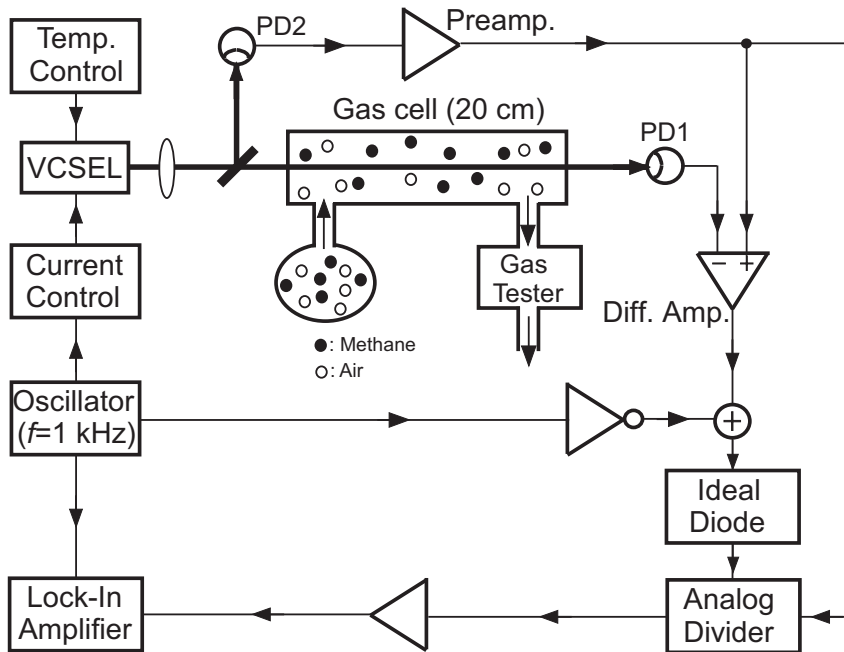
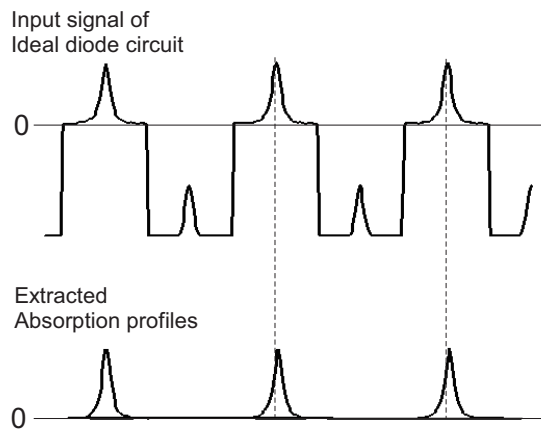Fig. 7.   Experimental setup of the *f* detection system.



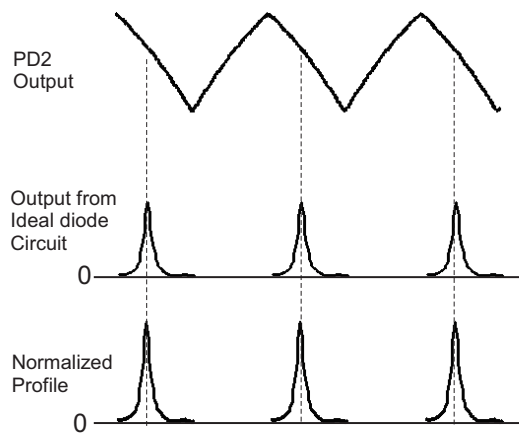Fig. 8.   Absorption profiles extracted from the combined signal by the ideal diode circuit.

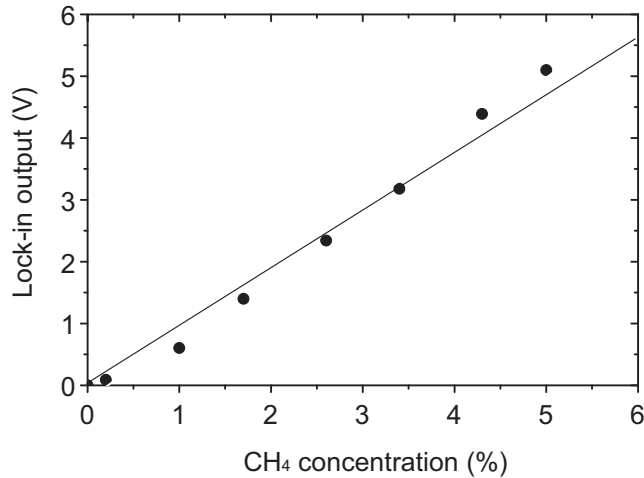Fig. 9.   Normalization of absorption profiles using the analogue divider.



Fig. 10.  Analytic line of $CH_4$ concentration (0 to 5%) obtained by the *f* system.

the line, lock-in amplifier output voltages can be transformed to $CH_4$ concentrations with a coefficient of approximately 1%/V.  Figure 11 shows the measured output voltages for seven different $CH_4$ concentrations, which are plotted as a function of the temperature drift of the VCSEL.  Unlike the data shown in Fig. 6, the output voltages are not significantly affected by the wavelength drift of the VCSEL, and the fluctuation decreased to less than 10% of that shown in Fig. 6.  Figure 12 shows the plot of temporal change in the lock-in output for 100 s (at 5% $CH_4$).  The resolution of the concentration, which is estimated from the root-mean-square of the fluctuations of the data, is better than 0.1%.
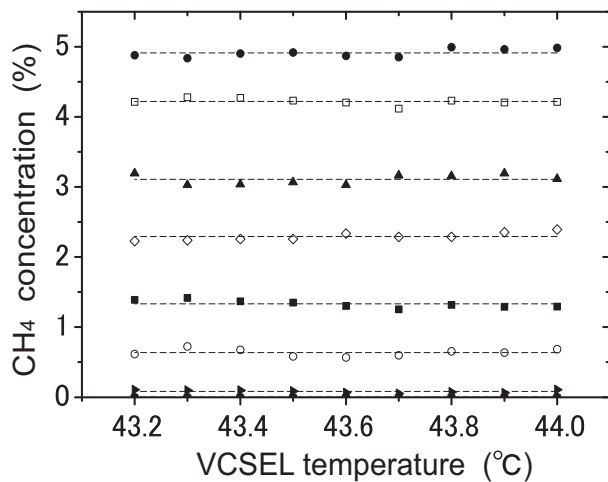
Fig. 11.  Measured $CH_4$ concentrations plotted as a function of VCSEL temperature.
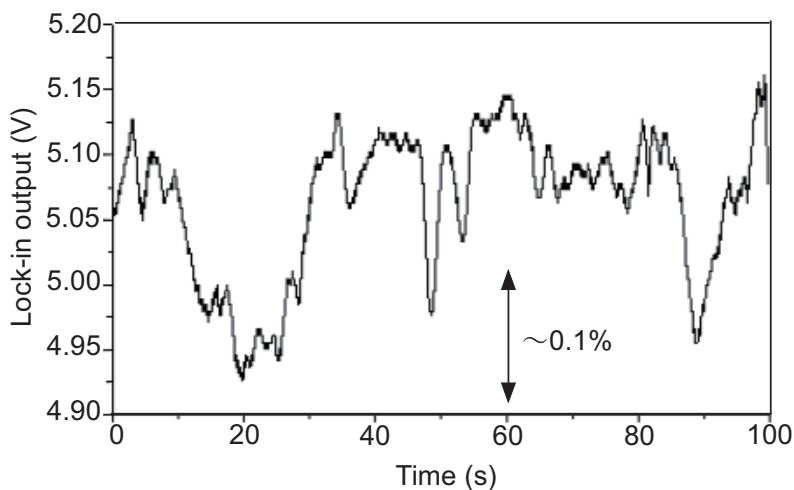


Fig. 12.  Temporal change of the lock-in output for 100 s (at 5% $CH_4$).

## 4.    Conclusions

In this work, we have developed a new practical technique for measuring $CH_4$ concentration in real time by introducing a VCSEL into the IR absorption method.  The method is based on the differential and synchronous detection of absorption lines and is unaffected by the wavelength drift of the light source.  As a result of our experiments, the analytic line was successfully obtained, and a concentration resolution of better than 0.1% was achieved.

# References

1  S. J. Gentry and P. T. Walsh: Sens. Actuators A, **5** (1984) 229.

2  J. Tamaki: Chem. Sensors **14** (1998) 163.

3  W. Shin, K. Imai, N. Izu and N. Murayama: Jpn. J. Appl. Phys., Part 2 **40** (2001) L1232.

4  S. Namba, K. Kawata, S. Nakajima and J. Tsuji: OUO BUTURI **26** (1957) 646 (in Japanese).

5  S. Tranchart, I. H. Bachir, and J.-L. Destombes: Appl. Opt. **35** (1996) 7070.

6  J. Wang, M. Maiorov, D. S. Baer, D. Z. Garbuzov, J. C. Connolly, and R. K. Hanson: Appl. Opt. **39** (2000) 5579.

7  K. Uehara and H. Tai: Appl. Opt. **31** (1992) 809.

8  M. C. Alarcon, H. Ito and H. Inaba: Appl. Phys. B **43** (1987) 79.

9  R. T. Wainner, B. D. Green, M. G. Allen, M. A. White, J. Stafford-Evans and R. Naper: Appl. Phys. B **75** (2002) 249.

10  K. Noda, M. Takahashi, R. Ohba and S. Kakuma: Opt. Eng. **44** (2005) 15.

11  T. Iseki, H. Tai and K. Kimura: Meas. Sci. Technol. **11** (2000) 594.

12  J. T. C. Liu, G. B. Rieker, J. B. Jeffries, M. R. Gruber, C. D. Carter, T. Mathur and R. K. Hanson: Appl. Opt. **44** (2005) 6701.

13  B. L. Fawcett, A. M. Parkes, D. E. Shallcross and A. J. Orr-Ewing: Phys. Chem. Chem. Phys. **4** (2002) 5960.

14  A. A. Kosterev and F. K. Tittel: Appl. Opt. **43** (2004) 6213.

15  L. S. Rothman, C. P. Rinsland, A. Goldman, S. T. Massie, D. P. Edwards, J.-M. Flaud, A. Perrin, C. Camy-Peyret, V. Dana, J.-Y. Mandin, J. Schroeder, A. Mccan, R. R. Gamache, R. B. Wattson, K. Yoshino, K. V. Chance, K. W. Jucks, L. R. Brown, V. Nemtchinov and P. Varanasi: J. Quant. Spectrosc. Radiat. Transfer **82** (2003) 5.

16  M. Young: Optics and Lasers, Including Fibers and Optical Waveguides (Springer-Verlag, Berlin, 1986).